Efficient biomass pretreatment using ionic liquids derived from lignin and hemicellulose

Aaron M. Socha[a,b,c], Ramakrishnan Parthasarathi[a,d], Jian Shi[a,d], Sivakumar Pattathil[e,f], Dorian Whyte[a,b,c], Maxime Bergeron[a], Anthe George[a,d], Kim Tran[a,d], Vitalie Stavila[d], Sivasankari Venkatachalam[e], Michael G. Hahn[e,f], Blake A. Simmons[a,d], and Seema Singh[a,d,1]

[a]Deconstruction Division, Joint BioEnergy Institute, Emeryville, CA 94608; [b]Center for Sustainable Energy and [c]Department of Chemistry and Chemical Technology, Bronx Community College, City University of New York, Bronx, NY 10453; [d]Biological and Materials Science Center, Sandia National Laboratories, Livermore, CA 94551; [e]Complex Carbohydrate Research Center, University of Georgia, Athens, GA 30602; and [f]The BioEnergy Science Center, Oak Ridge National Laboratory, Oak Ridge, TN 37831

Edited by Alexis T. Bell, University of California, Berkeley, CA, and approved July 9, 2014 (received for review March 27, 2014)

Ionic liquids (ILs), solvents composed entirely of paired ions, have been used in a variety of process chemistry and renewable energy applications. Imidazolium-based ILs effectively dissolve biomass and represent a remarkable platform for biomass pretreatment. Although efficient, imidazolium cations are expensive and thus limited in their large-scale industrial deployment. To replace imidazolium-based ILs with those derived from renewable sources, we synthesized a series of tertiary amine-based ILs from aromatic aldehydes derived from lignin and hemicellulose, the major by-products of lignocellulosic biofuel production. Compositional analysis of switchgrass pretreated with ILs derived from vanillin, *p*-anisaldehyde, and furfural confirmed their efficacy. Enzymatic hydrolysis of pretreated switchgrass allowed for direct comparison of sugar yields and lignin removal between biomass-derived ILs and 1-ethyl-3-methylimidazolium acetate. Although the rate of cellulose hydrolysis for switchgrass pretreated with biomass-derived ILs was slightly slower than that of 1-ethyl-3-methylimidazolium acetate, 90–95% glucose and 70–75% xylose yields were obtained for these samples after 72-h incubation. Molecular modeling was used to compare IL solvent parameters with experimentally obtained compositional analysis data. Effective pretreatment of lignocellulose was further investigated by powder X-ray diffraction and glycome profiling of switchgrass cell walls. These studies showed different cellulose structural changes and differences in hemicellulose epitopes between switchgrass pretreatments with the aforementioned ILs. Our concept of deriving ILs from lignocellulosic biomass shows significant potential for the realization of a "closed-loop" process for future lignocellulosic biorefineries and has far-reaching economic impacts for other IL-based process technology currently using ILs synthesized from petroleum sources.

renewable chemicals | bioenergy | lignocellulose conversion | saccharification | green chemistry

Room temperature ionic liquids (ILs) are commonly defined as molten salts with melting points less than 100 °C, and many ILs are considered environmentally friendly solvents for a variety of industrial applications. Their ionic, noncoordinating nature allows ILs to dissolve combinations of organic and inorganic compounds, facilitating diverse types of chemical transformation and separation processes (1, 2). ILs are often immiscible with organic solvents and thus provide nonaqueous alternatives for biphasic reaction systems, such as those involving homogeneous catalysts (3). In many cases, ILs are considered for "green chemistry" due to their low vapor pressures, high thermal stabilities, and relative nontoxicity. As such, they are emerging as important materials for drug delivery (4), lubrication (5), and electrolytes (6), including those for lithium ion (7) and lithium sulfur batteries (8). ILs have also found utility as heat transfer media for solar thermal systems (9), carbon capture (10), and biodiesel production (11). Among the industrial applications with highest potential volume requirements of these remarkable solvents is the processing of lignocellulosic biomass, and subsequent fermentation, to produce specialty and commodity chemicals including advanced biofuels (12–15).

Lignin and polysaccharides found in plant cell walls represent the two largest components of biomass on Earth, and it has been estimated that the United States has ∼1.3 billion tons of lignocellulosic biomass available per year (16). Lignin is a heterogeneous polymer that constitutes 20–30% of dry biomass in woody plants (17) and 15–20% in grasses (18). The monomeric composition of lignin comprises three primary phenylpropane units, *p*-coumaryl alcohol, coniferyl alcohol, and sinapyl alcohol, although this varies between species and the methods used for its extraction. Cellulose, a crystalline polymer of D-glucose, is the principal component of biomass, accounting for ∼40–50% of the dry biomass in woody plants and grasses (18, 19). Hemicellulose is a heterogeneous polymer of pentose and hexose sugars, and the composition of the hemicellulosic wall fraction varies significantly by species. Hemicelluloses account for ∼25% of the dry biomass of woody plants (20) and ∼30% of grasses (18).

Pretreatment of lignocellulosic biomass is a first step in either chemical or enzymatic depolymerization of the holocellulosic content of biomass. Approaches include steam explosion, high temperature treatment with addition of dilute acid or alkali; these have been reviewed extensively (21, 22). Although several methods can provide high yields of glucose and xylose, downstream

Significance

Ionic liquids (ILs) have unique properties applicable to a variety of industrial processes. Nearly universal solvating capabilities, low vapor pressures, and high thermal stabilities make these compounds ideal substitutes for a wide range of organic solvents. To date, the best performing ILs are derived from nonrenewable sources such as petroleum or natural gas. Due to their potential for large-scale deployment, ILs derived from inexpensive, renewable reagents are highly desirable. Herein, we describe a process for synthesizing ILs from materials derived from lignin and hemicellulose, major components of terrestrial plant biomass. With respect to overall sugar yield, experimental evaluation of these compounds showed that they perform comparably to traditional ILs in biomass pretreatment.

Author contributions: A.M.S., R.P., J.S., S.P., M.B., M.G.H., B.A.S., and S.S. designed research; A.M.S., R.P., J.S., S.P., D.W., M.B., A.G., K.T., V.S., and S.V. performed research; A.M.S., R.P., J.S., S.P., and M.B. contributed new reagents/analytic tools; A.M.S., R.P., J.S., S.P., D.W., M.B., A.G., M.G.H., B.A.S., and S.S. analyzed data; and A.M.S., R.P., J.S., S.P., M.G.H., B.A.S., and S.S. wrote the paper.

The authors declare no conflict of interest.

This article is a PNAS Direct Submission.

Freely available online through the PNAS open access option.

[1]To whom correspondence should be addressed. Email: seesing@sandia.gov.

This article contains supporting information online at www.pnas.org/lookup/suppl/doi:10.1073/pnas.1405685111/-/DCSupplemental.

fermentation of these sugars are often confounded by toxic byproducts (23). Due to their ability to selectively remove lignin and hemicellulose from biomass, effectively providing pure cellulose for enzymatic hydrolysis, certain ILs are exceptional pretreatment solvents (24–26). The most studied ILs are currently considered too expensive for large-scale biomass processing, typically require multistep syntheses, and are primarily derived from nonrenewable resources. For example, imidazole and pyridine, two of the best cation moieties for biomass pretreatment, are prepared industrially by the Radziszewski (27) and Chichibabin (28) condensation reactions, respectively. The starting materials for these syntheses include glyoxal and acetaldehyde, both of which are produced from ethylene obtained from petroleum cracking and/or hydraulic fracturing.

Imidazolium and other cations containing aromatic moieties have been shown to improve IL dissolution of wood (29–32). With this in mind, we turned our attention to the use of lignin- and hemicellulose-derived compounds as potential raw materials for IL synthesis. These polymers represent inexpensive and abundant waste streams from a variety of biomass-processing industries including textiles, pulp/paper, and biofuels. Chemical processes to produce ILs directly from biomass could lower costs by using large-volume, low-cost waste streams (Fig. 1). Critical to development of a "closed-loop" biorefinery is the controlled depolymerization of lignin and hemicellulose. Depending on the methods used, it is possible to direct depolymerization toward desired product streams, such as aromatic aldehydes, acids, and alcohols (33–35). For example, classic oxidative methods involving $CuSO_4$ with NaOH yield hydroxyl- and methoxyl-substituted aromatic aldehydes (36), particularly vanillin and syringaldehyde. A similar catalytic system, using $CuSO_4$ with quaternary ammonium and imidazolium dimethylphosphate ILs, has been shown to convert ~30% of lignin to aldehydes (37). Pyrolysis of lignin primarily produces aldehydes and phenols (33). Biological treatment of lignin by fungi of the genus *Pleurotus* has been shown to produce *p*-anisaldehyde as the dominant aromatic metabolite found in the culture broth (38). Aldehydes such as furfural and hydroxymethylfurfural can be derived in high yields from cellulose, hemicellulose, and untreated biomass (39). IL pretreatment of lignocellulosic biomass itself results in a small aromatics stream from lignin breakdown and could be potentially converted into renewable ILs (32).

We herein describe the first (to our knowledge) synthesis and evaluation of ILs from these lignin- and hemicellulose-derived compounds. Specifically, reductive amination chemistry was used to produce tertiary amines that were protonated with phosphoric acid to form the desired ILs. Dihydrogen phosphate containing ILs (**1–3**), were prepared from furfural, vanillin, and *p*-anisaldehyde, respectively. Combinations of computational and experimental methods were used to compare these compounds to 1-ethyl-3-methylimidazolium acetate, $[C_2mim][OAc]$ (**4**), an IL that has been well studied owing to its efficacy in biomass pretreatment (Fig. 2).

Results

Synthesis of ILs. Reductive amination of aldehydes derived from lignin and hemicellulose proceeded in excellent yields. A solution of the aldehyde was treated with diethylamine and sodium triacetoxyborohydride in 1,2-dichloroethane (40). A two-step acid/base workup provided the desired tertiary amine product without requiring any additional purification.

Furfural was first selected for reductive amination, as it is readily obtained from the acid-catalyzed dehydration of pentose sugars commonly found in hemicellulose. Its tertiary amine derivative, *N*-ethyl-*N*-(furanyl-2-methyl)ethanamine, was obtained in 82% yield. Vanillin and *p*-anisaldehyde were selected as lignin-derived aldehydes, and reductive amination provided their tertiary amine derivatives, 4-((diethylamino)methyl)-2-methoxyphenol and *N*-ethyl-*N*-(4-methoxybenzyl)ethanamine in 87% and 94% yield, respectively. The resulting amines were converted to ILs $[FurEt_2NH][H_2PO_4]$ (**1**), $[VanEt_2NH][H_2PO_4]$ (**2**), and $[p\text{-}AnisEt_2NH][H_2PO_4]$ (**3**) via stoichiometric addition of phosphoric acid in nearly quantitative yields (Fig. 3).

In all cases, ^1H NMR showed deshielding of methylene and methyl protons of the newly formed alkyl ammonium dihydrogen phosphate ILs, compared with those observed in the respective tertiary amines. For example, the methylene protons of the tertiary amine derived from furfural migrated downfield from $\delta = 2.41$ ppm to $\delta = 2.79$ ppm (q, 4H, $J = 8$ Hz) and from $\delta = 3.56$ ppm to $\delta = 4.09$ ppm (s, 2H) upon conversion to $[FurEt_2NH]$

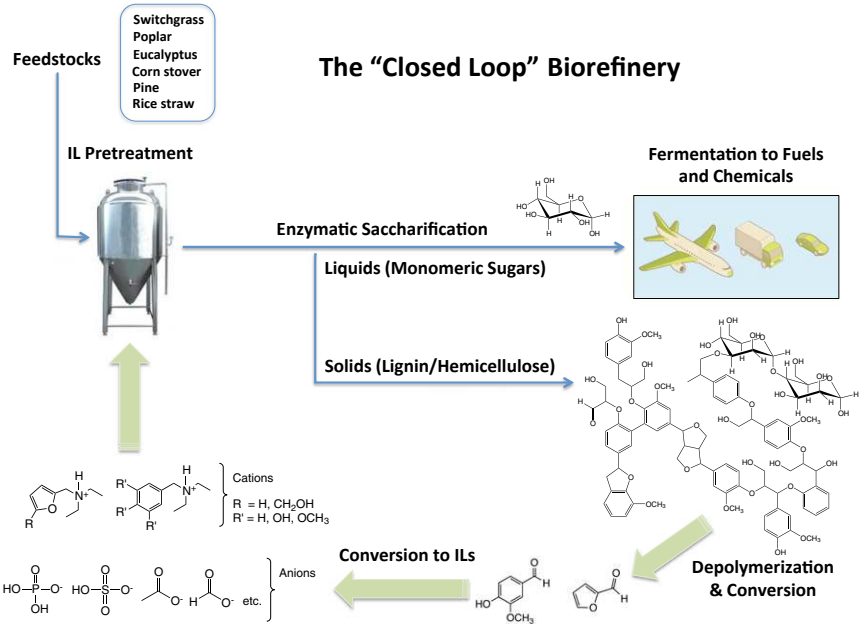

Fig. 1. Hypothetical process flow for a closed-loop biorefinery using ILs derived from lignocellulosic biomass.

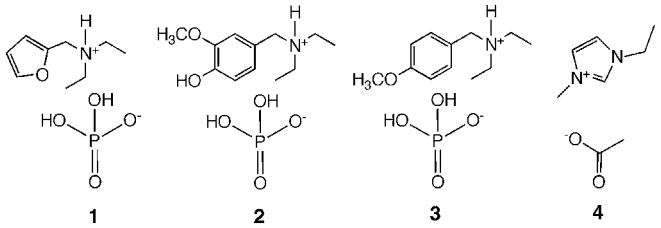

Fig. 2. Lignin- and hemicellulose-derived ILs evaluated in this study. [FurEt$_2$NH][H$_2$PO$_4$] (**1**), [VanEt$_2$NH][H$_2$PO$_4$] (**2**), and [*p*-AnisEt$_2$NH][H$_2$PO$_4$] (**3**) were prepared from furfural, vanillin, and *p*-anisaldehyde, respectively. IL **4** is [C$_2$mim][OAc].

[H$_2$PO$_4$]. A similar trend was observed for the equivalent protons of the methyl groups, shifting from δ = 0.99 ppm in the amine to δ = 1.19 ppm (t, 6H, J = 8 Hz) in the IL. Upon formation of [FurEt$_2$NH][H$_2$PO$_4$] from the tertiary amine, ^{13}C NMR revealed shielding effects on methyl carbon atoms, which shifted upfield from δ = 11.9 in the amine to δ = 9.7 ppm in the resulting IL. A slight shielding of the methylene carbons in the α position were also observed when converting the amine δ = 45.9 ppm (2C) and δ = 54.8 ppm (1C) to the IL δ = 45.3 ppm (2C) and δ = 54.6 ppm (1C). Similar chemical shift trends were observed for [VanEt$_2$NH][H$_2$PO$_4$] and [*p*-AnisEt$_2$NH][H$_2$PO$_4$], compared with their respective amines derived from vanillin and *p*-anisaldehyde. In total, these results compared well to model tertiary amines (41).

In addition to being among the most abundant representative aldehydes of chemically and biologically depolymerized lignin, respectively, [VanEt$_2$NH][H$_2$PO$_4$] and [*p*-AnisEt$_2$NH][H$_2$PO$_4$] were also selected based on their subtle differences in polarity and substituent effects. The polarity of an IL has been correlated with its ability to solubilize both lignin (42, 43) and cellulose (44–46). Hydroxyl and methoxyl groups activate aromatic ring systems, and therefore [VanEt$_2$NH][H$_2$PO$_4$] and [*p*-AnisEt$_2$NH][H$_2$PO$_4$] were used to dissect the role of these substituents on the relative acidity of the cation and relate these effects to biomass pretreatment.

Compositional Analysis of Untreated and Pretreated Switchgrass. Compositional analysis of cellulose, hemicellulose, and lignin was performed directly on the untreated switchgrass, and glucan and lignin values are in good agreement with previously published values (18, 47). The raw biomass contains 34.7% glucan, 21.8% xylan, and 19.3% lignin by mass (Table 1). The remaining biomass is likely a combination of cell wall components not detected by our methods, such as nonlignin phenolics, proteins, and arabinoglactans.

Switchgrass was pretreated at 160 °C with ILs synthesized from lignin and hemicellulose as well as our gold standard, [C$_2$mim][OAc], and subsequent compositional analysis was performed on biomass regenerated from reactions using water as the antisolvent. As expected, pretreatment increased the percent by mass of cellulose through the solubilization of lignin and hemicellulose. The benchmark IL for biomass pretreatment, [C$_2$mim][OAc] provided results consistent with previous studies, showing 58.0% biomass recovery, of which 55.2% was glucan, 20.8% was xylan, and 15.8% was lignin. This equates to 44.8% xylan and 52.4% lignin removal, respectively.

Of the lignin-based ILs tested, [VanEt$_2$NH][H$_2$PO$_4$] provided the highest solid recovery (77.9%) but performed poorest in terms of xylan and lignin removal, with 33.9% and 3.9%, respectively. It is hypothesized that because [VanEt$_2$NH][H$_2$PO$_4$] is the most polar IL, it is least suitable for lignin removal. The least polar biomass-derived IL, [*p*-AnisEt$_2$NH][H$_2$PO$_4$], showed far greater xylan and lignin removal, 51.4% and 43.0%, respectively, with total solid recovery of 56.7%. When comparing the monomeric sugar yields between [VanEt$_2$NH][H$_2$PO$_4$] and [*p*-AnisEt$_2$NH][H$_2$PO$_4$], it appears that the latter is a more promising candidate, as it provided 73.2% of the recovered biomass as glucan or xylan, compared with these combined sugar yields from [VanEt$_2$NH][H$_2$PO$_4$] pretreatment, being ∼65.7%.

Compositional analysis of switchgrass pretreated with [FurEt$_2$NH][H$_2$PO$_4$] showed 62.8% solid recovery, of which 52.5% was glucan and 17.8% was xylan. Significant xylan removal (48.8%) and lignin removal (20%) was observed for furfural-derived IL.

Performance of Biomass-Derived ILs for Biomass Pretreatment. From the compositional analysis, it was clear that 91–95% and 49–85% of the samples' glucan and xylan, respectively, were recovered in the solids. To liberate monomeric sugars (glucose and xylose) for downstream fermentation, enzymatic saccharification of this material was performed using a mixture of cellulase and endoxylanase enzymes. As expected, pretreatment with [C$_2$mim][OAc] provided >90% of the theoretical glucose and >70% of the theoretical xylose yields after a 24-h incubation with enzymes. Based on the compositional analysis, it was not surprising that [VanEt$_2$NH][H$_2$PO$_4$] gave only 50% glucose and <40% xylose yields at this time point.

Pretreatment with ILs [FurEt$_2$NH][H$_2$PO$_4$] and [*p*-AnisEt$_2$NH][H$_2$PO$_4$] gave >80% glucose and ∼60% xylose yields after the 24-h enzymatic saccharification period, and when the reaction was extended to 72 h, both compounds provided 90–95% glucose and 70–75% xylose yields. Although the hydrolysis rates were slower for biomass pretreated with [FurEt$_2$NH][H$_2$PO$_4$] and [*p*-AnisEt$_2$NH][H$_2$PO$_4$] ILs, they compared very well to [C$_2$mim][OAc] in terms of overall sugar yields (Fig. 4).

X-Ray Diffraction of Untreated and Pretreated Biomass. The proportions of crystalline cellulose (cellulose I) to amorphous cellulose (cellulose II) found in pretreated switchgrass samples were determined by powder X-ray diffraction. Because the biomass used in this study contained lignin and hemicellulose, crystallinity index (CrI) values were interpreted as relative comparisons. Untreated switchgrass had a CrI of 0.56 and showed major reflections at 22.5° and 15.7° 2θ, characteristic of the cellulose I polymorph, corresponding to [002] and combined [101] + [10$\bar{1}$] lattice places, respectively (48). A CrI of 0.22 accompanied by distortion in peak shape and shifts in position to ∼21° 2θ for the [002] lattice place and near disappearance of the combined [101] + [10$\bar{1}$] lattice places were observed for switchgrass pretreated with [C$_2$mim][OAc]. These changes are characteristic of the transition from cellulose I to cellulose II, and are commonly observed in biomass pretreated with [C$_2$mim][OAc] (49). Although [*p*-AnisEt$_2$NH][H$_2$PO$_4$]-pretreated switchgrass showed a slightly lower CrI (0.47), [FurEt$_2$NH][H$_2$PO$_4$] showed a CrI of 0.57 and all of the samples pretreated with biomass-derived ILs had 2θ peak shapes and positions similar to the untreated switchgrass (*SI Text*, section S3). The results show that cellulose decrystallization, as measured by CrI, is not a prerequisite for efficient enzymatic saccharification after pretreatment with [*p*-AnisEt$_2$NH][H$_2$PO$_4$] and [FurEt$_2$NH][H$_2$PO$_4$]. Cellulose accessibility, therefore,

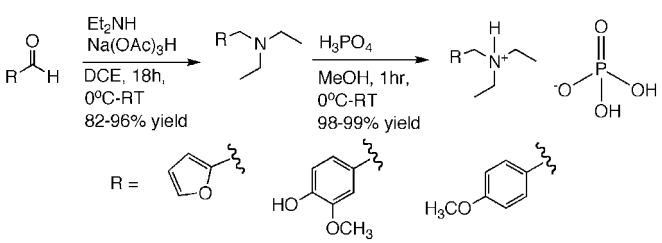

Fig. 3. Two-step synthesis to produce ILs from biomass-derived aldehydes.

Table 1. Composition analysis of IL-pretreated and untreated switchgrass

IL pretreatment	Solid recovery, %	Glucan, %	Xylan, %	Arabinan, %	Lignin, %	Xylan removal, %	Lignin removal, %
1 [$FurEt_2NH$][H_2PO_4]	62.8 ± 1.1	52.5 ± 0.7	17.8 ± 0.6	2.7 ± 0.1	24.6 ± 0.6	48.8	20.0
2 [$VanEt_2NH$][H_2PO_4]	77.9 ± 0.9	41.9 ± 0.4	23.8 ± 0.3	3.1 ± 0.1	23.8 ± 0.3	33.9	3.9
3 [*p*-$AnisEt_2NH$][H_2PO_4]	56.7 ± 1.7	54.5 ± 0.9	18.7 ± 0.3	3.0 ± 0.1	19.4 ± 0.9	51.4	43.0
4 [C_2mim][OAc]	58.0 ± 1.2	55.2 ± 0.5	20.8 ± 1.2	3.9 ± 0.1	15.8 ± 0.1	44.8	52.4
Untreated switchgrass	N/A	34.7 ± 1.3	21.8 ± 0.5	2.6 ± 0.4	19.3 ± 1.5	N/A	N/A

Note: ± indicates SD.

is likely affected by other factors such as lignin/hemicellulose content, porosity, and particle size (50). (See *SI Text*, section S3 and Fig. S1 for full experimental details.)

Solvation Parameters for Biomass-Derived ILs. Kamlet–Taft solvent parameters have been used to measure the ability of a solvent to donate a hydrogen bond (α), and accept a hydrogen bond (β) (51). It has been shown that basicity (β) correlates well with an IL's ability to dissolve lignocellulose (52), and that net basicity correlates with an IL's ability to dissolve cellulose (46, 53). A recent experimental study on a range of cations in combination with the same anion demonstrated that cation acidity is also important for cellulose dissolution (54). In the case of ILs [$VanEt_2NH$][H_2PO_4] and [*p*-$AnisEt_2NH$][H_2PO_4], one would expect the differential substitution of the electron-donating groups to affect the N atom's affinity for the H_3PO_4 proton. Molecular modeling was performed to estimate these effects.

Table 2 shows the calculated interaction energies (IEs) corrected with basis set superposition error correction and IL solvent parameters for ILs investigated here. The IEs for lignin-derived ILs are considerably higher in energy than [C_2mim][OAc]. Notably, all three biomass-derived ILs also have higher β values compared with [C_2mim][OAc]. The optimized geometries of ILs from biomass-derived aromatic aldehydes are shown in Fig. 5. In general, it can be seen from the IL geometries that the most stable conformation arises from interactions of an oxygen atom of the anion with the hydrogen atom on the nitrogen in the cation. Elongation of the N—H bond (from 1.1 to 1.5 Å) is noted in comparison with the isolated cation N—H bond distance (1.03 Å). Due to the significant elongation of the N—H bond in [$FurEt_2NH$][H_2PO_4], the hydrogen atom migrates to the oxygen atom of the anion, allowing strong intermolecular interactions between the IL cation and the anion.

The presence of a *para* hydroxyl group and a *meta* methoxyl groups in [$VanEt_2NH$][H_2PO_4] versus a *para* methoxyl group in [*p*-$AnisEt_2NH$][H_2PO_4], showed only slight differences in IEs and proton affinities, but significantly influenced the calculated solvent parameters. Comparison of the experimental results with the calculations of Kamlet–Taft solvent parameters of these ILs shows that effective pretreatment requires an IL with high hydrogen bond basicity and high net basicity. From Table 2, it can be seen that net basicity of [$FurEt_2NH$][H_2PO_4] and [*p*-$AnisEt_2NH$][H_2PO_4] ILs are higher than that of [C_2mim][OAc]. The comparatively lower proton affinities of the biomass-derived ILs compared with [C_2mim][OAc] could also provide hydrogen-bonding interactions with lignin, and delignification has been shown to significantly improve saccharification kinetics and yields (42). A computational comparison showed that the [$FurEt_2NH$]$^+$ cation had a stronger IE (28.8 kcal/mol) with a lignin model compound compared with the [C_2mim]$^+$ cation (21.4 kcal/mol). The model predicts that the proton of the [$FurEt_2NH$]$^+$ cation can form hydrogen bonds with ether linkages and hydroxyl oxygen atoms of lignin. (See *SI Text*, section S1 and Fig. S2, for full experimental details.) Combined, the compositional analysis and computational data from biomass-derived ILs suggest that high basicity and high net basicity are critical parameters required for efficient pretreatment.

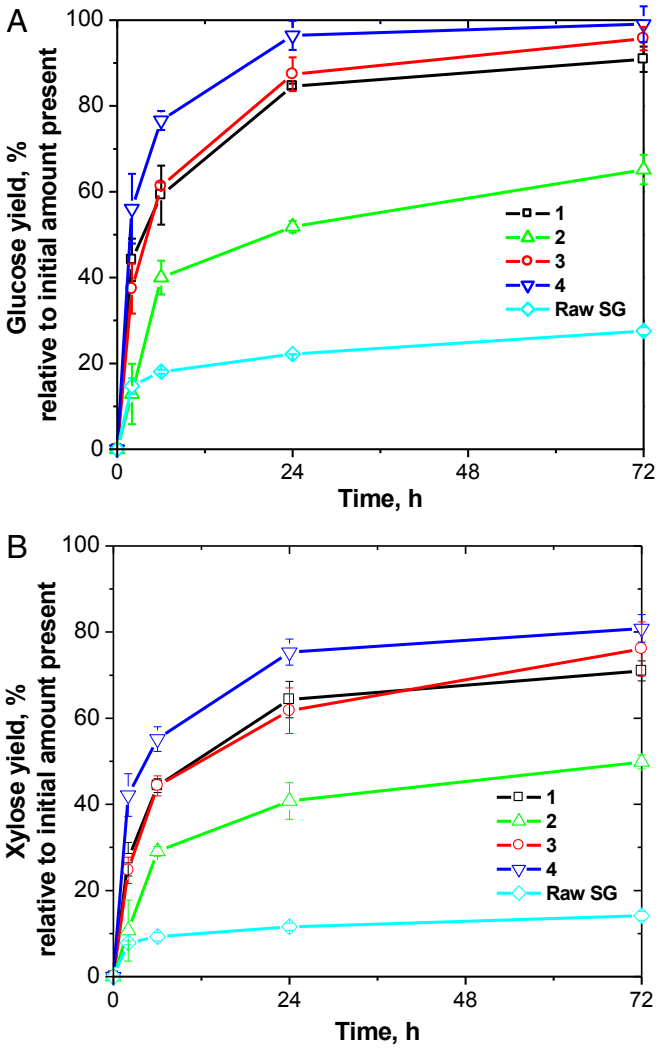

Fig. 4. Yields of glucose (*A*) and xylose (*B*) from untreated switchgrass (Raw SG) and switchgrass pretreated with [$FurEt_2NH$][H_2PO_4] (**1**), [$VanEt_2NH$][H_2PO_4] (**2**), [*p*-$AnisEt_2NH$][H_2PO_4] (**3**), and [C_2mim][OAc] (**4**).

Glycome Profiling of Untreated and IL-Pretreated Switchgrass. Glycome profiling of untreated switchgrass and switchgrass pretreated with either [$FurEt_2NH$][H_2PO_4], [*p*-$AnisEt_2NH$][H_2PO_4], or [C_2mim][OAc] was conducted to monitor changes in the overall composition and extractability of most major noncellulosic plant cell wall glycans. This method of analysis was performed to differentiate specific changes to biomass cell walls, and correlate those changes with reduced recalcitrance as a function of pretreatment.

Table 2. Calculated IE, proton affinity, acidity (α), basicity (β), and net basicity values of ILs evaluated in this study

Compound	IE, kcal/mol	Proton affinity (base), kcal/mol	α, eV	β, eV	Net basicity
[$FurEt_2NH$][H_2PO_4] (**1**)	165.51	233	2.14	3.53	1.39
[$VanEt_2NH$][H_2PO_4] (**2**)	118.14	234	2.35	2.99	0.63
[*p*-$AnisEt_2NH$][H_2PO_4] (**3**)	117.83	235	2.24	3.37	1.13
[C_2mim][OAc] (**4**)	106.42	257	2.28	2.97	0.69

Fig. 6 shows glycome profiles of untreated and IL-pretreated switchgrass. The profiles of the IL-pretreated switchgrass differed significantly from untreated switchgrass, emphasizing an overall change in the cell wall structure and integrity due to the solubilization and removal of lignin and lignin-associated carbohydrates during the pretreatment. The major changes in the profiles are highlighted as yellow dotted rectangles. The most dramatic changes in the glycome profiles were observed in the [$FurEt_2NH$][H_2PO_4]- and [*p*-$AnisEt_2NH$][H_2PO_4]-pretreated biomass samples. Both of these ILs removed essentially all of the arabinogalactan and homogalacturonan epitopes, and almost all of the xylan epitopes recognized by the xylan-3 through -5 groups of xylan-directed antibodies. The significant reduction observed in these epitopes from [$FurEt_2NH$][H_2PO_4]- and [*p*-$AnisEt_2NH$][H_2PO_4]-pretreated biomass samples may be due to two possible reasons. First, pretreatment conditions facilitated the removal of epitope structures from the corresponding glycans, and second, pretreatment caused significant cleavage of these cell wall glycans making their adsorption to the ELISA plates inefficient. It is also possible that a combination of these effects occurred. Pretreatment with [$FurEt_2NH$][H_2PO_4] and [*p*-$AnisEt_2NH$][H_2PO_4] also resulted in the loss of a substantial portion of the most tightly bound xyloglucan epitopes (4 M KOHPC extract) and a significant amount of the unsubstituted homoxylan epitopes recognized by the xylan-6 and -7 groups of antibodies. These latter epitopes became more extractable after pretreatment as indicated by the increased abundance of these xylan epitopes in the oxalate and carbonate extracts of the [$FurEt_2NH$][H_2PO_4]- and [*p*-$AnisEt_2NH$][H_2PO_4]-pretreated samples.

Pretreatment of switchgrass with [C_2mim][OAc] also led to a significant change in the glycome profile compared with the untreated biomass, but the changes are clearly distinct from those observed with the other two ILs. In particular, there was no apparent loss of xylan epitopes, but rather some xylans became more easily extractable and were observed in the oxalate and carbonate extracts, in contrast to the untreated biomass where almost no xylan epitopes were observed in these extracts. Enhanced extractability of xyloglucan epitopes was observed in switchgrass pretreated with [C_2mim][OAc]. In these samples, epitopes recognized by nearly all groups of xyloglucan-directed monoclonal antibodies were abundantly present in 1 M KOH extracts, compared with untreated switchgrass, while still being abundant in the 4 M KOH and 4 M KOHPC extracts. Loss of arabinogalactan epitopes was observed with [C_2mim][OAc] pretreatment, but this loss was not as extensive as was observed for the other two ILs. Finally, all homogalacturonan epitopes (recognized by the homogalacturonan backbone-1 group of monoclonal antibodies) were completely removed in all extracts of switchgrass pretreated with [C_2mim][OAc], as was the case with the other two ILs.

Pretreatment of switchgrass with any of the ILs also altered the amounts of material recovered in each extraction step. A marginal increase in the amount of carbohydrate materials recovered in the carbonate extracts was observed in the case of biomass pretreated with [$FurEt_2NH$][H_2PO_4] and [C_2mim][OAc]. In all IL-pretreated samples, relatively higher amounts of carbohydrate materials were released in 1 M KOH extracts compared with the untreated biomass. Correspondingly, notable reductions were observed in all IL-pretreated samples in terms of the amount of carbohydrates extracted with 4 M KOH. These results suggest an enhanced extractability of hemicellulosic glycans, which are the predominant alkali-extractable wall components in IL-pretreated samples. Earlier studies have shown that such increased hemicellulose extractability (particularly of xylans) is indicative of reduced recalcitrance (55).

Glycome profiling revealed significant changes in both glycan epitope content and extractability for IL-pretreated switchgrass compared with untreated switchgrass. Overall, the effects of the two biomass-derived ILs were different and more severe than the effects of [C_2mim][OAc]. The observed differences suggest a mechanism of action for [$FurEt_2NH$][H_2PO_4] and [*p*-$AnisEt_2NH$][H_2PO_4] that differs from that of [C_2mim][OAc]. (See *SI Text*, section S2 and Table S1 for full experimental details.)

Effect of Biomass-Derived ILs on Lignin–Carbohydrate Associations. Treatment of plant cell walls with chlorite cleaves and removes lignin, extracting all lignin-associated polysaccharides. The chlorite extracts from samples pretreated with [$FurEt_2NH$][H_2PO_4] and [*p*-$AnisEt_2NH$][H_2PO_4] was virtually devoid of all glycan epitopes, suggesting a significant reduction in lignin–polysaccharide associations in switchgrass subjected to pretreatment with these ILs. In contrast, the chlorite extracts from [C_2mim][OAc]-pretreated switchgrass, however, still contained significant amounts

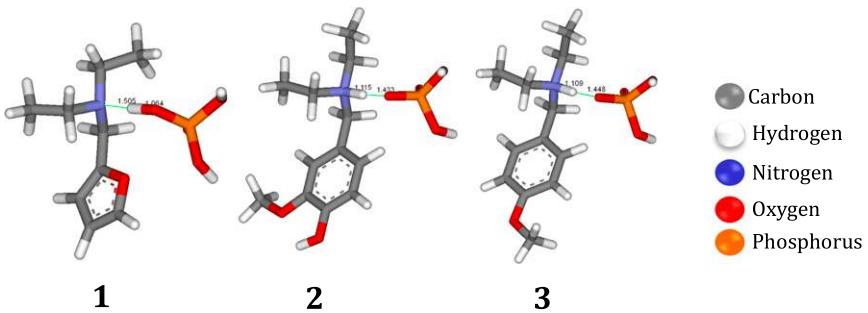

Fig. 5. Optimized geometries of [$FurEt_2NH$][H_2PO_4] (**1**), [$VanEt_2NH$][H_2PO_4] (**2**), and [*p*-$AnisEt_2NH$][H_2PO_4] (**3**) ILs evaluated in this study.

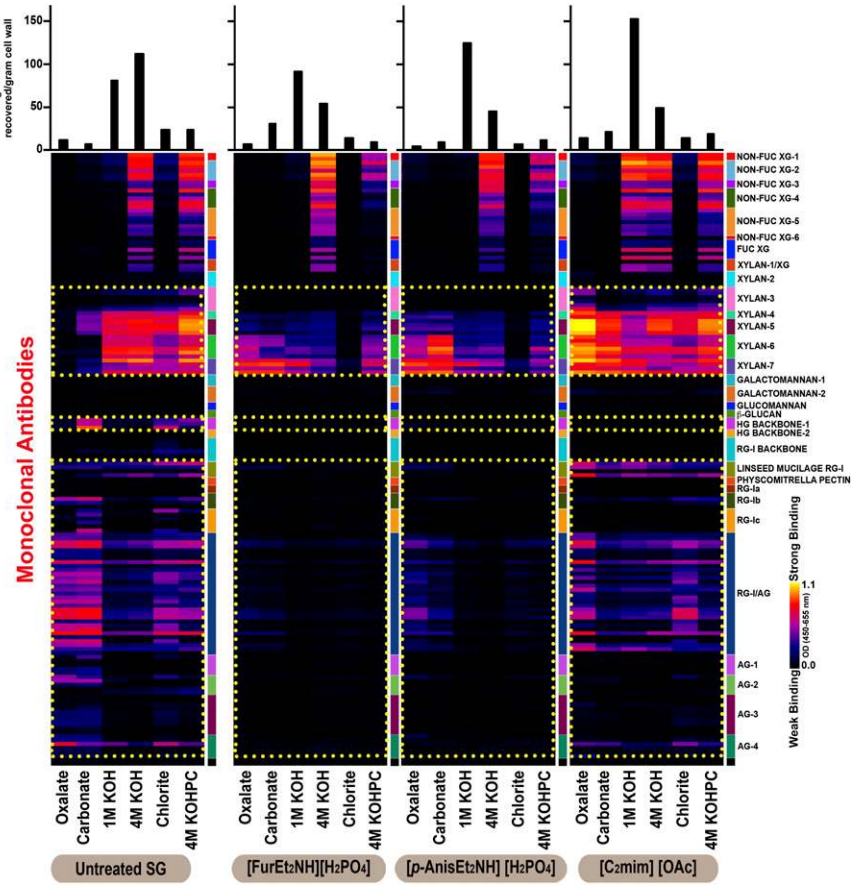

Fig. 6. Glycome profiling of untreated switchgrass (SG), and switchgrass pretreated with ILs [FurEt$_2$NH][H$_2$PO$_4$] (**1**), [*p*-AnisEt$_2$NH][H$_2$PO$_4$] (**3**), and [C$_2$mim][OAc] (**4**): Sequential cell wall extracts (*Bottom*) were subjected to ELISA screens with monoclonal antibodies for most major noncellulosic plant glycan classes (*Right*). The ELISA binding response values are represented as a color-coded heat map (*Center*), and the recovered masses of carbohydrate material resulting from each extraction step is represented with bar graphs (*Top*).

of xylans and pectic-arabinogalactan epitopes. Compositional analysis revealed that [C$_2$mim][OAc] removes greater amounts of lignin (52.4%) compared with [FurEt$_2$NH][H$_2$PO$_4$] (20.0%) and [*p*-AnisEt$_2$NH][H$_2$PO$_4$] (43.0%), suggesting that switchgrass pretreated with [C$_2$mim][OAc] may retain polysaccharides through other cell wall associations. There seems to be no such associations between lignin and xyloglucans in any of the ILs tested. Taken together, the above results provide further evidence that both [FurEt$_2$NH][H$_2$PO$_4$] and [*p*-AnisEt$_2$NH][H$_2$PO$_4$] reduce biomass recalcitrance through a similar mechanism, one that is significantly distinct from that of [C$_2$mim][OAc].

Cost Estimates. One important consideration for the proposed application for any IL is cost. A preliminary technoeconomic analysis (Table S2) based on raw materials cost for the biomass-derived ILs placed these compounds at approximately $12–15/kg. Replacement of diethylamine and Na(OAc)$_3$BH with NH$_3$ and H$_2$ for reductive amination (56) could significantly lower the raw materials cost to $4/kg. Although the methods and costs associated with the purification of aldehydes from depolymerized lignin and hemicellulose are still under investigation, there are industrial precedence for such processes and our results indicate that production of biomass-derived ILs holds significant promise. Current pricing estimates for [C$_2$mim][OAc] are approximately $17–25/kg.

Conclusions

We have shown the first (to our knowledge) synthesis and evaluation of a series of ILs from monomers obtained from lignin and hemicellulose. Reductive amination of these aromatic aldehydes followed by treatment with phosphoric acid provided three ILs in excellent yields without the need for chromatographic purification. Compositional analysis and sugar yields from enzymatic hydrolysis of pretreated switchgrass was used to compare these biomass-derived ILs to [C$_2$mim][OAc]. Enzymatic saccharification with [FurEt$_2$NH][H$_2$PO$_4$] and [*p*-AnisEt2NH][H$_2$PO$_4$] provided 90% and 96% of total possible glucose and 70% and 76% of total possible xylose, respectively, after biomass pretreatment. Of the three biomass-derived ILs, [FurEt$_2$NH][H$_2$PO$_4$] and [*p*-AnisEt2NH][H$_2$PO$_4$] also showed the highest β values, highest net basicity, and best ability to remove lignin. Computationally, [VanEt$_2$NH][H$_2$PO$_4$] showed the lowest net basicity and lignin removal efficiency, and the lowest sugar yields were observed experimentally. Compared with [C$_2$mim][OAc], we found that [FurEt$_2$NH][H$_2$PO$_4$] and [*p*-AnisEt$_2$NH][H$_2$PO$_4$] had substantially higher β and net basicity values and were less effective toward lignin removal. Sugar yields from switchgrass pretreated with these biomass-derived compounds, however, were nearly equivalent to yields from switchgrass pretreated with [C$_2$mim][OAc]. Taken together, compositional analysis and molecular modeling data suggest that lignin removal efficiency is a better indicator of switchgrass pretreatment performance compared with β and net basicity values when comparing benzylammonium and furfurylammonium ILs to those of imidazolium. These results are in agreement with previous findings in our group whereby choline-derived ILs with high lignin removal efficiency and high experimentally obtained β values resulted in high sugar yields across

a broad range of pretreatment temperatures (42). It is thought that the mechanism of action of the lignin- and hemicellulose-derived ILs is therefore more akin to other biologically derived ILs, such as ILs prepared from choline. Glycome-profiling experiments further suggested that the biomass-derived ILs [$FurEt_2NH$][H_2PO_4] and [*p*-$AnisEt_2NH$][H_2PO_4] act on plant cell walls in a mechanism distinct from [C_2mim][OAc], and studies are underway to understand these process implications in terms of lignin and hemicellulose depolymerization and IL recycling. These results indicate that biomass-derived ILs are very effective in biomass pretreatment and establish an important foundation for the further study of these unique compounds in other industrial applications.

Experimental Section

All solvents and chemicals were reagent grade and used without purification. NMR spectra were obtained on an Anasazi Eft-90 instrument (90 MHz for ^{1}H) in DMSO-d_6 and calibrated with tetramethylsilane for ^{1}H (δ = 0.00 ppm) and DMSO for ^{13}C (δ = 39.5 ppm), respectively (Fig. S3). Mass spectra were obtained on an Agilent 6890 GC equipped with an Agilent 5973 mass detector. Synthetic reactions were performed in triplicate, and average yields are reported.

Preparation of Tertiary Amines. ***N-Ethyl-N-(furan-2-ylmethyl)ethanamine.*** To a solution of furfural (10.0 g, 104 mmol, 1 equiv) in 1,2-dichloroethane (360 mL), cooled to 0 °C, was added diethylamine (18.3 g, 121 mmol, 1.2 equiv) and allowed to stir for 15 min. Sodium triacetoxyborohydride (30.9 g, 1.4 equiv) was added portionwise, and the mixture was stirred and allowed to warm to room temperature overnight under N_2. The solution was quenched by adding aqueous 3 M HCl and the amine product was thus drawn in the aqueous phase (pH ~1). The organic impurities were removed with the dichloroethane phase, and the aqueous phase was washed with CH_2Cl_2. The pH of the aqueous phase was raised to ~9.5 by addition of 3 M KOH, and the product was extracted two times with EtOAc. The combined organic layers are dried over Na_2SO_4 and concentrated to provide the product as a light brown liquid (13.1 g, 82% yield). All of the tertiary amine products below were prepared using this method. *m/z* [M^+] observed (Obsd.), 153.1, calculated (Calcd.), 153.12 for $C_9H_{17}NO$; ^{1}H NMR: 0.99 (t, 6H, *J* = 8 Hz), 2.41 (q, 4H, *J* = 8 Hz), 3.56 (s, 2H), 6.23 (m, 1H), 6.34 (m, 1H), 7.51 (m, 1H); ^{13}C NMR: 11.9 (2C), 46.3 (2C), 48.3, 107.9, 109.9, 141.8, 152.7.

4-((Diethylamino)methyl)-2-methoxyphenol. Following the general protocol for the reductive amination of aldehydes to tertiary amines, 15.0 g (100 mmol, 1 eq) of vanillin provided the desired product as a white amorphous solid (melting point, 75–77 °C; 18.3 g; 89% yield). *m/z* [M^+] Obsd., 209.1, Calcd., 209.14 for $C_{12}H_{19}NO_2$; ^{1}H NMR: 0.96 (t, 6H, *J* = 8 Hz), 2.43 (q, 4H, *J* = 8 Hz), 3.41 (s, 2H), 3.74 (s, 3H), 6.70 (s, 2H), 6.85 (s, 1H); ^{13}C NMR: 11.6 (2C), 46.0 (2C), 55.5, 56.9, 112.6, 115.1, 120.9, 130.6, 145.3, 147.4.

N-Ethyl-N-(4-methoxybenzyl)ethanamine. Following the general protocol for the reductive amination of aldehydes to tertiary amines, with 14.0 g (103 mmol, 1 eq) of *p*-anisaldehyde, provided the desired product as a pale yellow oil (19.0 g, 96% yield). *m/z* [M^+] Obsd., 193.1, Calcd., 193.15, for $C_{12}H_{19}NO$; ^{1}H NMR: 0.96 (t, 6H, *J* = 8 Hz), 2.43 (q, 4H, *J* = 8 Hz), 3.44 (s, 2H), 3.73 (s, 3H), 6.85 (d, $_{2H}$, *J* = 9 Hz), 7.22 (d, 2H, *J* = 9 Hz); ^{13}C NMR: 11.6 (2C), 45.9 (2C), 54.8, 56.3, 113.3 (2C), 129.5 (2C), 131.6, 158.2.

Preparation of ILs. ***N-Ethyl-N-(furan-2-ylmethyl)ethanamine, H_3PO_4 salt ([$FurEt_2NH$][H_2PO_4], 1).*** To a stirred 2 M solution of *N*-ethyl-*N*-(furan-2-ylmethyl)ethanamine (10.0 g, 65.0 mmol, 1 equiv) in MeOH (32.6 mL) at 0 °C was slowly added H_3PO_4 (6.4 g, 65.0 mmol, 1 equiv). The solution was allowed to stir, warming to room temperature for 3 h. Methanol was evaporated under vacuum and the IL **1** was obtained as a light brown liquid (16.0 g, 98% yield). All of the dihydrogen phosphate ILs described below were prepared by this method. ^{1}H NMR: 1.19 (t, 6H, *J* = 8 Hz), 2.79 (q, 4H, *J* = 8 Hz), 4.09 (s, 2H), 6.49 (m, 1H), 6.65 (m, 1H), 7.69 (m, 1H); ^{13}C NMR: 9.74 (2C), 46.4 (2C), 48.8, 111.1, 112.9, 144.2, 146.4.

4-((Diethylamino)methyl)-2-methoxyphenol, H_3PO_4 salt ([$VanEt_2NH$][H_2PO_4], 2). To a stirred 2 M solution of 4-((diethylamino)methyl)-2-methoxyphenol (10.0 g, 48.0 mmol, 1 equiv) in MeOH (23.9 mL) at 0 °C was slowly added H_3PO_4 (4.68 g, 48.0 mmol, 1 equiv). The solution was allowed to stir, warming to room temperature for 3 h. Methanol was evaporated under vacuum and the IL **2** was obtained as a pale pink crystals (melting point, 155–157 °C; 14.4 g; 98% yield). ^{1}H NMR: 1.09 (t, 6H, *J* = 8 Hz), 2.70 (q, 4H, *J* = 8 Hz), 3.74 (s, 2H), 3.78 (s, 3H), 6.78 (s, 2H), 7.07 (s, 1H); ^{13}C NMR: 9.08 (2C), 45.2 (2C), 55.3, 55.9, 114.4, 115.5, 123.3 (2C), 147.2, 147.8.

N-Ethyl-N-(4-methoxybenzyl)ethanamine, H_3PO_4 salt ([p-$AnisEt_2NH$][H_2PO_4], 3). To a stirred 2 M solution of *N*-ethyl-*N*-(4-methoxybenzyl)ethanamine (10.0 g, 52.0 mmol, 1 equiv) in MeOH (25.9 mL) at 0 °C was slowly added H_3PO_4 (5.07 g, 52.0 mmol, 1 equiv). The solution was allowed to stir, warming to room temperature for 3 h. Methanol was evaporated under vacuum and the IL **3** was obtained as a viscous pale yellow oil (14.9 g, 99% yield). ^{1}H NMR: 1.18 (t, 6H, *J* = 8 Hz), 2.85 (q, 4H, *J* = 8 Hz), 3.77 (s, 3H), 4.00 (s, 2H), 6.95 (d, 1H, *J* = 10 Hz), 7.52 (d, 2H, *J* = 8 Hz); ^{13}C NMR: 9.1 (2C), 45.3, 48.8, 54.6, 55.2, 114.1 (2C), 124.7, 132.1 (2C), 160.0.

Biomass Pretreatment. Four hundred milligrams of dry switchgrass were mixed with 3.6 g of ILs and 0.4 mL of water to give a 10 wt% biomass loading in tubular reactors made of 0.75-inch-diameter × 6-inch-length stainless-steel (SS316) tubes and sealed with stainless-steel caps. All pretreatment reactions were run in triplicate. Tubular reactors were heated to 160 °C in convention oven. The heat-up time was ~10 min and the reactions were run for 3 h after the desired temperature was reached. After pretreatment, the reactors were allowed to cool to room temperature. The mixture of IL, water, and pretreated biomass was transferred to a 50-mL Falcon tube using deionized (DI) water to a final volume of 25 mL and then centrifuged at 3,220 × *g* to separate the solid and liquid phases. An aliquant of supernatant was taken for lignin and sugar analysis. The solid fraction was washed sequentially with 40 mL of hot water, 40 mL of 1:1 acetone:water, and three times with 40 mL of hot water to remove any residual IL and/or sugars. Washed solids were lyophilized in a FreeZone Freeze Dry System (Labconco) for composition analysis and enzymatic saccharification.

Enzymatic Saccharification. Enzymatic saccharification of untreated and pretreated samples were run in triplicate following National Renewable Energy Laboratory Laboratory Analytical Procedure 9 "Enzymatic Saccharification of Lignocellulosic Biomass" standard conditions (50 °C, 0.05 M citrate buffer, pH 4.8) (57). Citrate buffer (final molarity, 50 mM), sodium azide (antimicrobial, final concentration of 0.02 g/L), enzymes, and DI water were mixed with pretreated solids to achieve a final solid loading of ~10%. Enzyme loadings were calculated from compositional analysis data. Fifteen milligrams of CTec2 (batch number VCN10001) per gram of untreated biomass and 1.5 mg of HTec2 (batch number VHN00001) per gram of glucan were used. The protein content of enzymes was measured by bicinchoninic acid (BCA) assay with a Pierce BCA Protein Assay Kit (Thermo Scientific) using BSA as protein standard. CTec2 has a protein content of 186.6 ± 2.0 mg/mL, whereas HTec2 contains 180.1 ± 1.8 mg/mL protein. The enzyme mixtures were gifts from Novozymes N.A. An aliquot of supernatant was taken at 2, 6, 24, and 72 h and was analyzed by HPLC for monosaccharide content as described previously (58). Glucose yield was calculated from the maximum potential glucose available from glucan in pretreated biomass.

Glycome Profiling. To conduct glycome profiling, alcohol-insoluble residues of cell walls derived from untreated and IL-pretreated switchgrass were subjected to sequential extractions using increasingly harsh reagents (59). In the case of native plant cell walls, mild conditions such as oxalate and carbonate extracts, remove the most loosely bound pectic polysaccharides. Alkaline treatment with 1 M KOH removes more tightly bound pectin and hemicelluloses that mainly comprise xylan and pectin, and 4 M KOH extracts xyloglucans in addition to xylan and pectins. Treatment with acetic acid/chlorite at high temperature (chlorite extraction) breaks down most of the lignin, releasing lignin-associated polysaccharides into this fraction. Finally, a 4 M KOHPC treatment removes any residual polysaccharides that remain bound to the cell wall via association with lignin. To facilitate glycome profiling, all extracts were probed with a comprehensive suite of cell wall glycan-directed monoclonal antibodies, and the binding responses of these monoclonal antibodies are represented as color-coded "heat maps" (59). The total amounts of carbohydrates recovered under each extraction condition were also quantified gravimetrically and are represented as bar graphs atop Fig. 6. (See *SI Text*, section S2 and Table S1 for full experimental details.)

Computational Details and Theoretical Development of Hydrogen-Bonding Acidity and Basicity Descriptors. The geometry optimizations of three ionic liquids (ILs), [$FurEt_2NH$][H_2PO_4] (**1**), [$VanEt_2NH$][H_2PO_4] (**2**), and [*p*-$AnisEt_2NH$][H_2PO_4] (**3**), were performed using density functional theory (DFT) with the M06-2X hybrid exchange-correlation functional and the 6-311++G(d, p) basis set. Frequency calculations were carried out to verify that the computed structures corresponded to energy minima. Interaction energies were calculated to measure the binding strength between cation and anion of ILs and corrected for basis set superposition error:

$$IE = -[E_{IL} - (E_{anion} + E_{cation})] \quad [1]$$

where E_{IL} refer to the energies of cation and anion pair (for IL), and E_{anion} and E_{cation} refer to the energies of the anion and cation monomer molecule,

respectively. In the present study, DFT-based global reactivity descriptors, such as chemical hardness, chemical potential, and electrophilicity were calculated (60). Quantum chemical reactivity descriptors predicted acidity, basicity, and net basicity, and showed good correlation with experimentally observed values for [C_2mim][OAc] (**4**). These results provide a basis to describe the observed experimental delignification trend for a set of ILs (42). These descriptors were used to derive the molecular basicity, acidity, and net basicity values for the [C_2mim][OAc] and biomass derived ILs. According to the DFT (61), the chemical potential (μ), and chemical hardness (η) are defined as follows:

$$\chi = -\mu = -\left(\frac{\partial E}{\partial N}\right)_{v(\vec{r})} \quad [2]$$

and

$$\eta = \frac{1}{2}\left(\frac{\partial^2 E}{\partial N^2}\right)_{v(\vec{r})} = \frac{1}{2}\left(\frac{\partial \mu}{\partial N}\right)_{v(\vec{r})}, \quad [3]$$

where E is the total energy of the system, N is the number of electrons in the system, and $v(\vec{r})$ is the external potential. μ is identified as the negative of the electronegativity (χ). By applying finite difference approximation to Eqs. **2** and **3**, we get the operational definition for η and μ as follows:

$$\mu = -\frac{(IP + EA)}{2}, \quad [4]$$

$$\eta = \frac{IP - EA}{2}. \quad [5]$$

Chemical potential and chemical hardness can be rewritten using Koopmans' theorem in terms of the vertical ionization potential and electron affinity as follows:

$$\eta = \frac{E_{LUMO} - E_{HOMO}}{2}, \quad [6]$$

$$\mu = \frac{E_{LUMO} + E_{HOMO}}{2}, \quad [7]$$

where E_{LUMO} is the lowest unoccupied molecular orbital's energy and E_{HOMO} is the highest occupied molecular orbital's energy.

Upon formation of a hydrogen bond, electron density is transferred from the hydrogen bond acceptor toward the hydrogen bond donor. In the light of the "hard and soft acids and bases" concept (62), the propensity of molecule to donate the electron density depends inversely on the electronegativity and hydrogen atom-attracting sites are formed through the interaction of intramolecular sites of different electronegativity. Hence, we define the hydrogen-bonding basicity B^{IL} of an IL using a simple working equation based on DFT-based descriptors as follows:

$$B^{IL} = \eta^2/\chi. \quad [8]$$

An increased electrostatic component and the high electronegativity of a molecule influences the hydrogen-bonding ability. In the case of basicity, electronegativity is very important for hydrogen bonding. Therefore, molecular acidity dependence on the reduced orbital electronegativity of the molecule is considered. The formula for the acidity is written as follows:

$$A^{IL} = \chi^2/2\eta. \quad [9]$$

IL net basicity values were reported as a difference in $B^{IL} - A^{IL}$. Proton affinity values were calculated at M06-2X/6-311++G(d, p) level from the cationic conjugated acids and neutral unconjugated bases for ILs **1–4**. All quantum chemical calculations were performed using the Gaussian 09 suite of programs (63).

ACKNOWLEDGMENTS. We thank Novozymes for their generous donation of Ctec2 and Htec2 enzymes, and Christian Rodriguez [Bronx Community College (BCC)] for his kind assistance with NMR measurements. This work conducted by the Joint BioEnergy Institute was supported by the Office of Science, Office of Biological and Environmental Research, US Department of Energy, under Contract DE-AC02-05CH11231. Additional funding was provided by Research Foundation, City University of New York (65102-00 43). This research used resources of the National Energy Research Scientific Computing Center and BCC. The glycome profiling was supported by the BioEnergy Science Center administered by Oak Ridge National Laboratory and funded by Grant DE-AC05-00OR22725 from the Office of Biological and Environmental Research, Office of Science, US Department of Energy. The generation of the CCRC series of plant cell wall glycan-directed monoclonal antibodies used in this work was supported by the National Science Foundation Plant Genome Program (DBI-0421683 and IOS-0923992).

1. Welton T (1999) Room temperature ionic liquids. Solvents for synthesis and catalysis. *Chem Rev* 99(8):2071–2084.
2. Brennecke J, Maginn E (2001) Ionic liquids: Innovative fluids for chemical processing. *AIChE J* 47(11):2384–2389.
3. Giernoth R (2007) Homogeneous catalysis in ionic liquids. *Top Curr Chem* 276:1–23.
4. Stoimenovski J, MacFarlane DR, Bica K, Rogers RD (2010) Crystalline vs. ionic liquid salt forms of active pharmaceutical ingredients: A position paper. *Pharm Res* 27(4): 521–526.
5. Bermúdez MD, Jiménez AE, Sanes J, Carrión FJ (2009) Ionic liquids as advanced lubricant fluids. *Molecules* 14(8):2888–2908.
6. Galiński M, Lewandowski A, Stępniak I (2006) Ionic liquids as electrolytes. *Electrochim Acta* 51(26):5567–5580.
7. Lewandowski A, Swiderska-Mocek A (2009) Ionic liquids as electrolytes for Li-ion batteries—an overview of electrochemical studies. *J Power Sources* 194(2):601–609.
8. Park JW, et al. (2013) Ionic liquid electrolytes for lithium-sulfur batteries. *J Phys Chem C* 117(40):20531–20541.
9. Mills D (2004) Advances in solar thermal electricity technology. *Sol Energy* 76:19–31.
10. Shannon MS, Bara JE (2011) Reactive and reversible ionic liquids for CO_2 capture and acid gas removal. *Sep Sci Technol* 47(2):178–188.
11. Fauzi AHM, Amin NAS (2012) An overview of ionic liquids as solvents in biodiesel synthesis. *Renew Sustain Energy Rev* 16:5770–5786.
12. Stark A (2011) Ionic liquids in the biorefinery: A critical assessment of their potential. *Energy Environ Sci* 4:19–32.
13. Bokinsky G, et al. (2011) Synthesis of three advanced biofuels from ionic liquid-pretreated switchgrass using engineered *Escherichia coli*. *Proc Natl Acad Sci USA* 108(50):19949–19954.
14. Li C, et al. (2010) Comparison of dilute acid and ionic liquid pretreatment of switchgrass: Biomass recalcitrance, delignification and enzymatic saccharification. *Bioresour Technol* 101(13):4900–4906.
15. Shi J, et al. (2012) Impact of mixed feedstocks and feedstock densification on ionic liquid pretreatment efficiency. *Biofuels* 4(1):63–72.
16. Simmons BA, Loque D, Blanch HW (2008) Next-generation biomass feedstocks for biofuel production. *Genome Biol* 9(12):242.
17. Kilpeläinen A, et al. (2003) Wood properties of Scots pines (*Pinus sylvestris*) grown at elevated temperature and carbon dioxide concentration. *Tree Physiol* 23(13):889–897.
18. Perez-Pimienta JA, et al. (2013) Comparison of the impact of ionic liquid pretreatment on recalcitrance of agave bagasse and switchgrass. *Bioresour Technol* 127:18–24.
19. Kostiainen K, et al. (2008) Wood properties of trembling aspen and paper birch after 5 years of exposure to elevated concentrations of CO_2 and O_3. *Tree Physiol* 28(5): 805–813.
20. Schädel C, Blöchl A, Richter A, Hoch G (2010) Quantification and monosaccharide composition of hemicelluloses from different plant functional types. *Plant Physiol Biochem* 48(1):1–8.
21. Mosier N, et al. (2005) Features of promising technologies for pretreatment of lignocellulosic biomass. *Bioresour Technol* 96(6):673–686.
22. Wyman CE, et al. (2005) Coordinated development of leading biomass pretreatment technologies. *Bioresour Technol* 96(18):1959–1966.
23. Palmqvist E, Hahn-Hägerdal B (2000) Fermentation of lignocellulosic hydrolysates. I: Inhibition and detoxification. *Bioresour Technol* 74:17–24.
24. Pu Y, Jiang N, Ragauskas AJ (2007) Ionic liquid as a green solvent for lignin. *J Wood Chem Technol* 27(1):23–33.
25. Binder JB, Raines RT (2009) Simple chemical transformation of lignocellulosic biomass into furans for fuels and chemicals. *J Am Chem Soc* 131(5):1979–1985.
26. Lee SH, Doherty TV, Linhardt RJ, Dordick JS (2009) Ionic liquid-mediated selective extraction of lignin from wood leading to enhanced enzymatic cellulose hydrolysis. *Biotechnol Bioeng* 102(5):1368–1376.
27. Ebel K, et al. (2012) Imidazole and derivatives: Section 4.1—the Radziszewski reaction. *Ullmann's Encyclopedia of Industrial Chemistry* (Wiley, New York), pp 638–639.
28. Kirk RE, Othmer DF (2005) *Kirk-Othmer Encyclypedia of Chemical Technology J*, eds Kroschwitz I, Seidel A (Wiley, New York), p 16.
29. Kilpeläinen I, et al. (2007) Dissolution of wood in ionic liquids. *J Agric Food Chem* 55(22):9142–9148.
30. Singh S, Simmons BA, Vogel KP (2009) Visualization of biomass solubilization and cellulose regeneration during ionic liquid pretreatment of switchgrass. *Biotechnol Bioeng* 104(1):68–75.
31. Arora R, et al. (2010) Monitoring and analyzing process streams towards understanding ionic liquid pretreatment of switchgrass (*Panicum virgatum*). *BioEnergy Res* 3:134–145.
32. Varanasi P, et al. (2013) Survey of renewable chemicals produced from lignocellulosic biomass during ionic liquid pretreatment. *Biotechnol Biofuels* 6(1):14.
33. Pandey MP, Kim CS (2011) Lignin depolymerization and conversion: A review of thermochemical methods. *Chem Eng Technol* 34(1):29–41.
34. Kleen M, Gellerstedt G (1991) Characterization of chemical and mechanical pulps by pyrolysis-gas chromatography/mass spectrometry. *J Anal Appl Pyrolysis* 19:139–152.

35. Xiang Q, Lee YY (2000) Oxidative cracking of precipitated hardwood lignin by hydrogen peroxide. *Appl Biochem Biotechnol* 84–86(1-9):153–162.
36. Pearl IA (1942) Vanillin from lignin materials. *J Am Chem Soc* 64(6):1429–1431.
37. Liu S, et al. (2013) Process of lignin oxidation in ionic liquids coupled with separation. *RSC Adv* 3(17):5789–5793.
38. Gutiérrez A, Caramelo L, Prieto A, Martínez MJ, Martínez AT (1994) Anisaldehyde production and aryl-alcohol oxidase and dehydrogenase activities in ligninolytic fungi of the genus *Pleurotus*. *Appl Environ Microbiol* 60(6):1783–1788.
39. Binder JB, et al. (2009) Reactions of lignin model compounds in ionic liquids. *Biomass Bioenergy* 33:1122–1130.
40. Abdel-Magid AF, Carson KG, Harris BD, Maryanoff CA, Shah RD (1996) Reductive amination of aldehydes and ketones with sodium triacetoxyborohydride. studies on direct and indirect reductive amination procedures. *J Org Chem* 61(11):3849–3862.
41. Pretsch E, Bühlmann P, Affolter C (2000) *Structure Determination of Organic Compounds* (Springer, Berlin), pp 121–122, 208.
42. Sun N, et al. (2014) Understanding pretreatment efficacy of four cholinium and imidazolium ionic liquids by chemistry and computation. *Green Chem* 16:2546–2557.
43. Brandt A, et al. (2013) Deconstruction of lignocellulosic biomass with ionic liquids. *Green Chem* 15:550–583.
44. Fukaya Y, et al. (2008) Cellulose dissolution with polar ionic liquids under mild conditions: Required factors for anions. *Green Chem* 10(1):44–46.
45. Ohno H, Fukaya Y (2009) Task specific ionic liquids for cellulose technology. *Chem Lett* 38(1):2–7.
46. Hauru LK, Hummel M, King AW, Kilpeläinen I, Sixta H (2012) Role of solvent parameters in the regeneration of cellulose from ionic liquid solutions. *Biomacromolecules* 13(9): 2896–2905.
47. Samuel R, et al. (2011) Structural changes in switchgrass lignin and hemicelluloses during pretreatments by NMR analysis. *Polym Degrad Stabil* 96(11):2002–2009.
48. Segal L, et al. (1962) An empirical method for estimating the degree of crystallinity of native cellulose using the x-ray diffractometer. *Text Res J* 29:786–794.
49. Cheng G, et al. (2012) Impact of ionic liquid pretreatment conditions on cellulose crystalline structure using 1-ethyl-3-methylimidazolium acetate. *J Phys Chem B* 116(33):10049–10054.
50. Park S, Baker JO, Himmel ME, Parilla PA, Johnson DK (2010) Cellulose crystallinity index: Measurement techniques and their impact on interpreting cellulase performance. *Biotechnol Biofuels* 3(10):10.
51. Kamlet M, Abboud J, Taft R (1977) The solvatochromic comparison method. 6. The .pi.* scale of solvent polarities. *J Am Chem Soc* 99(18):6027–6038.
52. Brandt A, et al. (2010) The effect of the ionic liquid anion in the pretreatment of pine wood chips. *Green Chem* 12(4):672–679.
53. Parviainen A, et al. (2013) Predicting cellulose solvating capabilities of acid-base conjugate ionic liquids. *ChemSusChem* 6(11):2161–2169.
54. King AWT, et al. (2012) Relative and inherent reactivities of imidazolium-based ionic liquids: The implications for lignocellulose processing applications. *RSC Adv* 2(21): 8020–8026.
55. Pattathil S, et al. (2012) Changes in cell wall carbohydrate extractability are correlated with reduced recalcitrance of HCT downregulated alfalfa biomass. *Ind Biotechnol (New Rochelle N Y)* 8(4):217–221.
56. Gomez S, Peters JO, Maschmeyer T (2002) The reductive amination of aldehydes and ketones and the hydrogenation of nitriles: Mechanistic aspects and selectivity control. *Adv Synth Catal* 344(10):1037–1057.
57. Sluiter A, et al. (2005) *Determination of Structural Carbohydrates and Lignin in Biomass* (National Renewable Energy Laboratory, Golden, CO).
58. Shi J, et al. (2013) One-pot ionic liquid pretreatment and saccharification of switchgrass. *Green Chem* 15:2579–2589.
59. Pattathil S, Avci U, Miller JS, Hahn MG (2012) Immunological approaches to plant cell wall and biomass characterization: Glycome profiling. *Methods Mol Biol* 908:61–72.
60. Chattaraj PK, Sarkar U, Roy DR (2006) Electrophilicity index. *Chem Rev* 106(6): 2065–2091.
61. Parr RG, Yang W (1989) *Density Functional Theory of Atoms and Molecules* (Oxford Univ Press, Oxford).
62. Pearson RG, Songstad J (1967) Application of the principle of hard and soft acids and bases to organic chemistry. *J Am Chem Soc* 89(8):1827–1836.
63. Frisch MJ, et al. (2009) *Gaussian 09* (Gaussian, Inc., Wallingford, CT), Revision A.01.